



# A Life Cycle Assessment Study of Acid Mine Drainage Treatment Using Steel Dust Mineralization Products

Reza Mahmoudi Kouhi<sup>1,2</sup> · Faramarz Doulati Ardejani<sup>1,2,3</sup> · Sied Ziaedin Shafaei Tonkaboni<sup>1</sup> · Mohammad Milad Jebrailvand Moghaddam<sup>1,2</sup> · Christoph Butscher<sup>4</sup> · Reza Taherdangkoo<sup>4</sup>

Received: 14 January 2024 / Accepted: 20 August 2024 / Published online: 3 December 2024  
© The Author(s) 2024

## Abstract

Mining and its associated industries contribute to greenhouse gas (GHG) emissions, exacerbating climate change. To address this, our study employed life cycle assessment to assess the carbon footprint of utilizing carbonates made from steel dust from the Golgohar complex in a carbon mineralization process to treat acid mine drainage (AMD) at the Darreza copper mine. We considered four scenarios and two sensitivity analyses, including the baseline scenario, solar energy utilization, dust variations, limestone purchase, transportation impact, and AMD quantity. The baseline scenario yielded a negative carbon footprint of  $-107 \text{ kg of CO}_2\text{eq}/100 \text{ kg of CO}_2$  from flue gas. Using solar energy prevented most of the GHG emissions. In addition, using a waste with high alkalinity reduced energy consumption throughout the process. Furthermore, the utilization of trucks with high capacity for product transportation and treating a low amount of AMD improved the entire process and kept it in the negative carbon footprint range. Finally, comparing scenarios to the conventional use of purchased limestone for AMD treatment demonstrated environmental viability. The study demonstrates the potential for sustainable practices in mining, promoting a shift towards methods that would mitigate environmental impact and contribute to a more carbon-neutral future.

**Keywords** LCA · AMD · Carbon mineralization · Carbon footprint · Sustainability

---

✉ Reza Taherdangkoo  
reza.Taherdangkoo@ifgt.tu-freiberg.de

Reza Mahmoudi Kouhi  
reza\_mahmoudi@ut.ac.ir

Faramarz Doulati Ardejani  
fdoulati@ut.ac.ir

Sied Ziaedin Shafaei Tonkaboni  
Zshafaei@ut.ac.ir

Mohammad Milad Jebrailvand Moghaddam  
milad.jebrailvand@ut.ac.ir

Christoph Butscher  
Christoph.Butscher@ifgt.tu-freiberg.de

## Introduction

Effective greenhouse gas (GHG) emission management is essential for mining-related industries to reduce their impacts on climate change (Azadi et al. 2019; Liu et al. 2021). Furthermore, the importance of these measures extends to resource efficiency and compliance with environmental regulations. Mining companies can reduce their environmental footprint, improve operational efficacy, and maintain their social acceptance and authorization for operation by taking specific actions, such as the incorporation of carbon utilization strategies (Lesser et al. 2021). Carbon utilization is a procedure that aims to capture carbon dioxide ( $\text{CO}_2$ ) emissions from either atmospheric (Wang and Song 2020) or industrial sources (Hunt et al. 2010) and convert them into valuable products or materials (Al-Mamoori et al. 2017; Zhang et al. 2020). One approach to carbon utilization is carbon mineralization, where  $\text{CO}_2$  reacts with metal cations (Romanov et al. 2015) to produce stable and non-toxic carbonate minerals (Gadikota 2021). In-situ mineralization involves injecting  $\text{CO}_2$  into geological formations containing alkaline minerals (Kelemen et al. 2018),

<sup>1</sup> School of Mining, College of Engineering, University of Tehran, Tehran, Iran

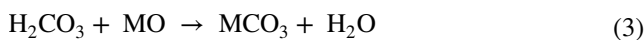
<sup>2</sup> Climate Change Group, Mine Environment and Hydrogeology Research Laboratory (MEHR Lab.), University of Tehran, Tehran, Iran

<sup>3</sup> Head of Mine Environment and Hydrogeology Research Laboratory (MEHR Lab.), University of Tehran, Tehran, Iran

<sup>4</sup> TU Bergakademie Freiberg, Institute of Geotechnics, Gustav-Zeuner-Str. 1, 09599 Freiberg, Germany

while ex-situ mineralization uses alkaline industrial waste or mine tailings on the Earth's surface (Kelly et al. 2011; Rim et al. 2020). Both methods are a way to reduce GHG emissions by permanently storing CO<sub>2</sub> in carbonate minerals.

Moreover, there are two approaches to ex-situ mineralization: indirect and direct carbonation. Indirect carbonation is used for unrefined solid materials and is more energy-efficient and cost-effective than direct carbonation; however, it can have some serious environmental side effects. In this method, acids or other solvents are used to extract reactive components from minerals, and these components react with CO<sub>2</sub> in either an aqueous or a gaseous phase. This approach can be divided into several categories, including gas–solid carbonation, where the mineral is first converted into an oxide or hydroxide and then carbonates (Eftekhari et al. 2023; Siyar et al. 2022; Teir 2008). Direct carbonation, on the other hand, involves either direct gas–solid carbonation or aqueous mineral carbonation. Direct gas–solid carbonation is the simplest method, but it has some fundamental difficulties, such as a slow reaction rate and applicability to only refined materials, such as calcium and magnesium oxides and hydroxides. In contrast, aqueous mineral carbonation is the most commonly studied ex-situ mineral carbonation route, and it involves CO<sub>2</sub> interacting with metal oxide minerals, typically magnesium and calcium silicates in an aqueous solution at high pressure (Bobicki et al. 2012; Madadgar et al. 2023; Sanna et al. 2014). This approach involves the dissolution of CO<sub>2</sub> in water to form carbonic acid (H<sub>2</sub>CO<sub>3</sub>), which then reacts with metal oxide minerals to form stable metal carbonates. The overall reaction for aqueous mineral carbonation is given in Eq. 1. In this reaction, CO<sub>2</sub> reacts with water and metal oxide minerals (MO) to produce metal carbonates (MCO<sub>3</sub>) and water. The metal oxide minerals typically used in this reaction are magnesium and calcium silicates, as they are abundant in nature and have a high reactivity with CO<sub>2</sub>. The first step in the carbonation reaction is illustrated in Eq. 2. When CO<sub>2</sub> is dissolved in water, it reacts with water to form H<sub>2</sub>CO<sub>3</sub> through a reversible reaction. This reaction is important because it allows CO<sub>2</sub> to be more easily transported and dissolved in water, which is necessary for the carbonation reaction. The second step in the carbonation reaction is shown in Eq. 3. The carbonic acid is reacted with the metal oxide minerals to produce metal carbonates and water (Metz et al. 2005; Tatomir et al. 2018; Teir 2008).



Ex-situ mineralization commonly uses waste materials from various industries such as steel (Ibrahim et al. 2019a), coal sectors (Reddy et al. 2011), and aluminum

(Endzhievskaya et al. 2020) manufacturing facilities as feedstock. These waste materials contain substantial amounts of alkaline earth metals, especially calcium and magnesium, which are useful in the mineralization process (Pan et al. 2020). Steel production byproducts, such as steel dust, are particularly important due to their high concentrations of metals and minerals, including calcium and magnesium. Steel dust is generated during the smelting and refining of steel scrap and is present in the flue gas and waste streams of steel mills. This material can react with CO<sub>2</sub> to create stable carbonates (El-Naas et al. 2015; Ibrahim et al. 2019b). Therefore, using these materials can be an effective way of implementing ex-situ mineralization for carbon capture, utilization, and storage.

In addition, acid mine drainage (AMD) is acidic and often rich in metals (Akçil and Koldas 2006). It is primarily formed when sulfide minerals such as pyrite, marcasite, pyrrhotite, and chalcopyrite undergo chemical and biological oxidation. In the past 60 years, various active and passive methods have been implemented to remediate and treat AMD, but the success of these methods depends on the quality and quantity of AMD, as well as the formation and settling of metal hydroxides. While active treatment systems involve direct contact between acidic and alkaline materials, such as limestone or lime, to neutralize the acidity of the mine drainage (Skousen et al. 2000, 2019), passive treatment systems utilize natural processes, such as bacterial reactions, wetlands, aeration, and dissolution of limestone, to neutralize the acidity of the mine water and remove trace elements (Skousen et al. 2017).

Previous studies have investigated the environmental impacts of AMD treatment using LCA. Moreno-González et al. (2023) conducted a life cycle analysis on various management strategies for metal-rich sludge from AMD treatment. Martínez et al. (2019) used LCA to evaluate different environmental impacts of passive remediation of AMD. Hengen et al. (2014) assessed various passive and active AMD treatment approaches using LCA. In another study, Tuazon and Corder (2008) compared the use of seawater-neutralized red mud and lime to treat AMD by LCA. In addition, there has been some LCA research on carbon mineralization using alkaline materials, particularly steel slag. For example, Li et al. (2021) used LCA to compare CO<sub>2</sub> capture of steel slag products. Ostovari et al. (2020) utilized LCA to compare the carbon footprint of mineralization using alkaline materials such as steel slag and olivine. However, the carbon footprint of AMD treatment using steel dust as an alkaline agent in a mineralization process remains unaddressed. Our motivation was to address both the environmental concerns of greenhouse gas emissions from mining operations and the environmental issues of AMD through LCA.

## LCA Methodology

The life cycle assessment (LCA) methodology assesses the environmental impact of a product or process across its full life cycle in four steps: goal definition, inventory analysis, impact assessment, and interpretation (Hauschild et al. 2018). In this section, the four steps of LCA related to this study will be presented in detail.

### Goal and Scope Definition

The first step of LCA, goal and scope definition, sets study objectives, including the functional unit, system boundaries, and assumptions, ensuring focus, relevance, and consistency (Rebitzer et al. 2004; Hauschild et al. 2018). This study aims to assess the carbon footprint of treating AMD from the Darreza copper mine using alkaline dust from the Golgohar iron complex by means of carbon mineralization.

### Functional Unit

In LCA, the functional unit allows consistent comparisons among products or processes by measuring the system's output, forming the basis for comparing alternatives (de Simone Souza et al. 2021). The chosen functional unit in this study is 100 kg of CO<sub>2</sub> derived from flue gas. Although other functional units, such as the weight of produced carbonates, were feasible choices, this specific functional unit enabled us to compare our results with those from previous mineralization studies.

### System Boundary

The LCA's system boundary defines the study's scope from extraction to disposal, focusing on relevant inputs and outputs, and excluding irrelevant stages (Hauschild et al. 2018; Tillman et al. 1994). The scope of this study encompassed the incorporation of input materials such as steel dust, AMD, and flue gas within its system boundary. The upstream environmental impacts of these materials from the extraction to waste storage were assumed to be zero. This is because ISO 14040 outlines principles, including "allocation," where reusing or recycling waste in a process can be considered to have minimal or zero impact (ISO 14040 2006). The carbonates were first produced as valuable materials and were then considered waste after being used to treat AMD. Materials that exit the system boundary at different stages were categorized as waste too, because implementing a detailed LCA for waste disposal would have broadened the scope of the study and could have reduced the focus on the primary research questions. Moreover, comprehensive LCA studies often face

limitations due to the lack of detailed inventory data. However, all of the necessary heat and electricity for the diverse processes were taken into account in this study (Fig. 2). This study also considered the avoided impacts caused by the heat and alkaline products. Conversely, the system boundary omitted elements such as the impacts associated with device construction, human activities, and labor, and the maintenance and repair of devices and facilities.

### Analysis Assumption

In LCA, assumptions bridge data gaps, ensuring completeness and accuracy despite incomplete information across a product or process's life cycle (Hauschild et al. 2018). The assumptions used in this study are given below.

- The iron present in the steel dust was removed after a stage of gravity separation. This assumption is based on the fact that extensive and successful projects have been carried out at the Golgohar iron complex to extract iron from tailings using proper methods such as gravity separation, and the factory has a comprehensive plan for this purpose.
- The reaction in this study occurs with near-complete efficiency. This common assumption is based on the fact that the reaction efficiency can vary depending on various factors such as the reaction conditions, the quality of the reagents, and the presence of impurities. Nevertheless, contrary to other research, like that of Yan et al. (2021), every alkaline component was deemed non-inert. This characteristic enhances the accuracy of the study, especially regarding calculations involving energy and heat.
- The heat generated from the performed exothermic reactions in this study is fully stored and used for other reactions that require heat. This assumption is based on the fact that the heat generated during the exothermic reactions can be utilized in other processes.

### Life Cycle Inventory

Life cycle inventory (LCI), the second stage of LCA, gathers data on materials, energy, emissions, and waste throughout a product or process's life cycle to create an inventory of inputs and outputs (Martínez-Rocamora et al. 2016; Ross and Evans 2002). LCI data in LCA comes from different sources: primary from manufacturers, secondary from databases or literature, and simulation when primary or secondary data is missing, estimating the inventory (Guo and Murphy 2012; Hauschild et al. 2018). The LCI of this study included primary and secondary data, such as the characteristics of the steel dust (Table 1), obtained from the factory, and the AMD (Table 2), which was obtained from published literature. It also includes data obtained through

**Table 1** Characteristics of the Golgohar steel dust

Compound	Value (kg)
SiO <sub>2</sub>	118.28
MgO	73.25
CaO	28.47

**Table 2** Characteristics of the AMD from the Darreza copper mine (Shahabpour and Keshavarzi 2006)

Compound	Value (mg/L)
Na	30.4
Ca	204
Mg	24
Cl <sup>−</sup>	639
Cu	52
Fe	11
Mn	1.24
K	3.9
SO <sub>4</sub> <sup>2−</sup>	561.5
pH	3.44

simulation, such as materials and energy for different stages of the process. Moreover, this research incorporated the Ecoinvent database to supplement the missing data for the inventory analysis and calculating the carbon footprint of different products (Supplemental Table S-1).

### Life Cycle Impact Assessment

Life cycle impact assessment (LCIA), the subsequent stage in LCA, assesses environmental impacts by quantifying various factors like climate change, resource depletion, and human toxicity throughout a product's or process's life cycle. Methods like Eco-indicator 99, ReCiPe, IPCC, and CML convert collected inventory data from the LCI stage into impact scores for evaluation (Renou et al. 2008; Rosenbaum et al. 2018). In this LCA study, the IPCC GWP100a impact assessment method was used as the LCIA method. This is a recognized and accepted method for evaluating the impact of GHG emissions on global warming potential. Using a widely accepted impact assessment method like IPCC also allows for easy comparison of results with similar studies in the future, promoting transparency and consistency. The other reason for choosing this single indicator method, rather than using more comprehensive methods such as Eco-indicator 99 or ReCiPe, is that the database for this method is smaller, more accurate, and more accessible.

### Interpretation

Interpretation is the last stage of an LCA study where the results of the previous stages are analyzed and conclusions are drawn (Sala et al. 2020). This stage aims to understand

environmental impacts and identify areas for improvement. It involves analyzing results in line with study objectives and scope (Hauschild et al. 2018; Rebitzer et al. 2004).

### Simulation

The treatment of AMD by steel dust was simulated using DWSIM, an open-source chemical process simulation software. DWSIM is widely used for its comprehensive features that allow for the simulation of chemical processes, making it an ideal tool for our LCA study. This software supports detailed thermodynamic modeling, advanced unit operations, and extensive process design capabilities, which are crucial for simulating the complex interactions in our study. The main DWSIM databases used in this study were ChemSep and Electrolytes. The chemical abstracts service (CAS) numbers of components not available in these databases were added.

Using the data obtained from this section, which is a subset of the collected data, the LCI stage was completed, and the study entered the LCIA stage. This simulation was divided into four different steps: CO<sub>2</sub> extraction, dust hydration, carbonate production, and AMD treatment, which are colored red, blue, green, and black, respectively, in Fig. 1. Together, the first three steps comprise mineral carbonation.

In the first step, the CO<sub>2</sub> is extracted from the factory's flue gas. The flue gas is reacted with chemicals such as monoethanolamine to obtain pure CO<sub>2</sub>. The input volumes were adjusted to yield an output close to 100 kg of CO<sub>2</sub>, which was the functional unit of this study. Initially, the flue gas (FLU) and the reactive chemicals (MEA +) are fed into a separator (SEP1), where they react. The output of this step is in the form of a gas phase (G1-) and a liquid phase (FLUMEA). The gas phase (G1-) then enters a vapor–liquid separator (VLS1) to be further separated into liquid (LIQ1-) and gas (VPR1-) phases before being removed from the system as waste. However, the liquid phase (FLUMEA) continues along its path and is fed into a pump (PUMP1) and then a heater (HEATER1) to be prepared for the main separation stage with greater pressure and temperature. There, the liquid phase is again divided into liquid (MEA-) and gas (CON-CO<sub>2</sub>) phases using another separator (SEP2). The gas phase contains high-purity CO<sub>2</sub> and the liquid phase comprises other compounds such as monoethanolamine present in the feed, which is removed from the system as a waste. The CO<sub>2</sub> output stream is then fed into a compressor (CMP), making it ready to be used in the third step.

In the dust hydration step, a combination of steel dust and water outflow from the factory is used to produce Ca(OH)<sub>2</sub> and Mg(OH)<sub>2</sub>. In the process shown in Fig. 1, 220 kg (Table 1) of the dust from the Golgohar steel complex (DUSTGOL) and 250 kg of salt water outflow from the same

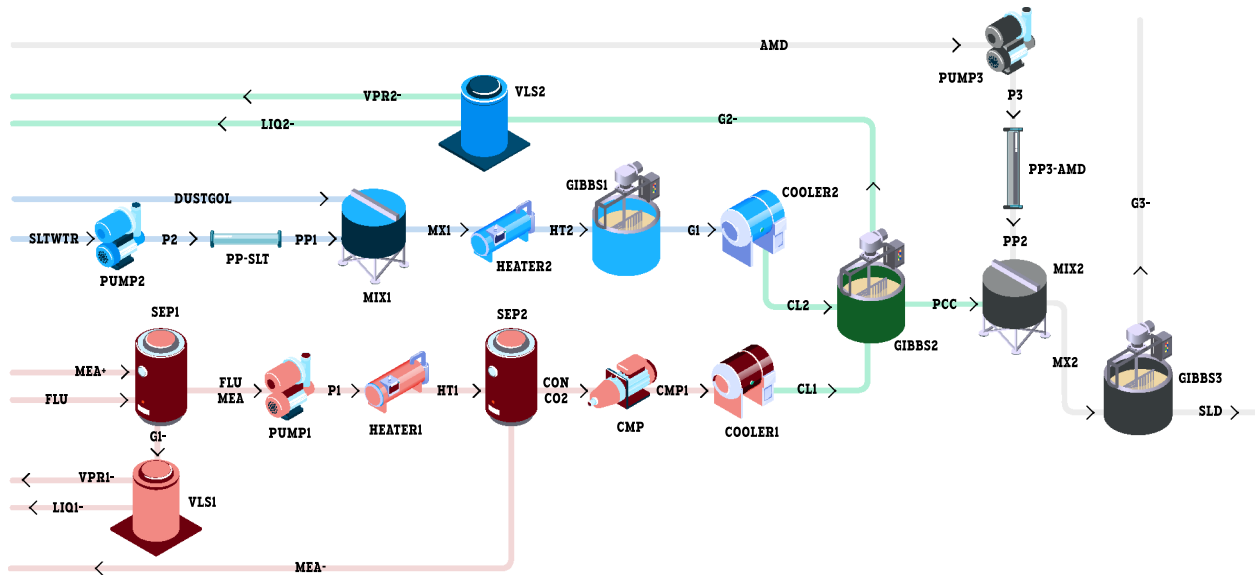
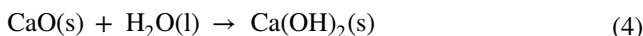


**Fig. 1** Simulation steps of CO<sub>2</sub> extraction (red), dust hydration (blue), carbonate production (green), and AMD treatment (black) (designed by Freepik)

factory are mixed (MIX1) and then heated (HEATER2) to prepare the materials for reaction in the GIBBS1 apparatus. The purpose of this process is to convert CaO and MgO into Ca(OH)<sub>2</sub> and Mg(OH)<sub>2</sub> (Eqs. 4 and 5; (El-Naas et al. 2015)), which are more effective substances for reacting with CO<sub>2</sub> to form carbonates.



In the third stage, the output streams of the previous two stages, namely the  $\text{Ca}(\text{OH})_2$ ,  $\text{Mg}(\text{OH})_2$ , and pure  $\text{CO}_2$  are used to produce carbonates (Eq. 6 and Eq. 7; (El-Naas et al. 2015)). The last stream of the first step (CMP1), which contains pure  $\text{CO}_2$ , is cooled down (CL1) then enters another reaction apparatus (GIBBS2). Meanwhile, the prepared stream of the second step (CL2) also enters that apparatus and reacts with the  $\text{CO}_2$  after cooling (COOLER2), to form carbonates. The output of this step is in both liquid and solid forms. The liquid phase (G2-) enters a vapor–liquid separator (VLS2) to be precisely separated into gas and liquid phases, before being removed from the system as a waste. The solid phase containing the formed carbonates is ready to react with the AMD in the following stages.



In the fourth step, the aforementioned carbonate products react with the AMD of the Darreza copper mine (Table 2).

neutralizing the acid and precipitating its excessive elements. At first, mixing occurs between the pumped AMD (P3) and the produced carbonates in a mixer (MIX2). Then, in the last reaction apparatus (GIBBS3), the AMD and carbonates react with each other. In the final stage, the solid materials (SLD) (resulting alkaline waste) and liquid ones (G3) (the treated AMD) are discharged from the two outputs of this device, both as waste.

## Scenarios and Sensitivity Analysis

LCA studies benefit from applying many scenarios and sensitivity analyses to determine their impact on the environment. This strategy aids stakeholders in making informed, long-term decisions by identifying crucial factors, trade-offs, and increasing credibility. The aim of using different scenarios and sensitivity analyses in this study was to examine the changes in the carbon footprint resulting from modifications in different parts of the process and ultimately compare the scenarios to determine the best course of action. In the following section, four implemented scenarios and two sensitivity analysis will be discussed.

## Scenario #1: Baseline Scenario

The baseline scenario under consideration in this study involved the use of steel dust and flue gas from the Golgohar complex, as well as AMD from the Darreza mine, as input materials. It also involved using wastewater from the Golgohar complex to supply the required water as well

as using fossil fuels as the main source for providing heat and electricity throughout the process, since this is the most common energy source for industries in Iran. Choosing this scenario as the baseline case is based on its likelihood of being the most feasible and executable condition for both factories. The system boundary of this scenario is shown in Fig. 2. It should be noted that in this scenario, it was assumed that the Darreza copper mine is located next to the Golgohar iron complex. In the first sensitivity analysis, the distance between these two mines and the impact of product transportation by trucks was examined.

### Scenario #2: Use of Solar Energy

The second scenario in this study involved using solar energy as a source of heat (not electricity) for reactions rather than the conventional source described in the baseline scenario. The central region of Iran, where most of the large-scale mines, such as Golgohar, are located, is a favorable location for solar energy utilization due to its high levels of solar irradiation (Alamdar et al. 2013). Solar thermal systems are generally more efficient and cost-effective for certain applications that require heat and the technology for converting solar energy into electricity is not yet widely available

or affordable in that area (Ahmadi et al. 2018; Herez et al. 2016). However, the choice of whether to use solar energy for heat, electricity, or both will depend on several factors, including the availability and cost of technology, and the specific needs and goals of the industry and local communities. The results from this scenario and its comparison with other scenarios can be important in making informed decisions about the best approach to reduce the site's carbon footprint and increase the mining industry's sustainability, particularly given the need to review the use of fossil fuels and reduce GHG emissions.

### Scenario #3: Use of the Emirates Steel Plant Dust

This scenario involves the use of dust from the Emirates steel plant (El-Naas et al. 2015). The lower levels of calcium and magnesium in the dust from the Golgohar steel company, compared to other alkaline residues (Bobicki et al. 2012), suggested that replacing it with a higher calcium and magnesium content residue could facilitate the production of more carbonates and reduce energy consumption, resulting in a lower carbon footprint. Therefore, the dust composition from the Emirates steel plant was substituted for Golgohar's dust in this scenario. It was assumed that the process takes place in

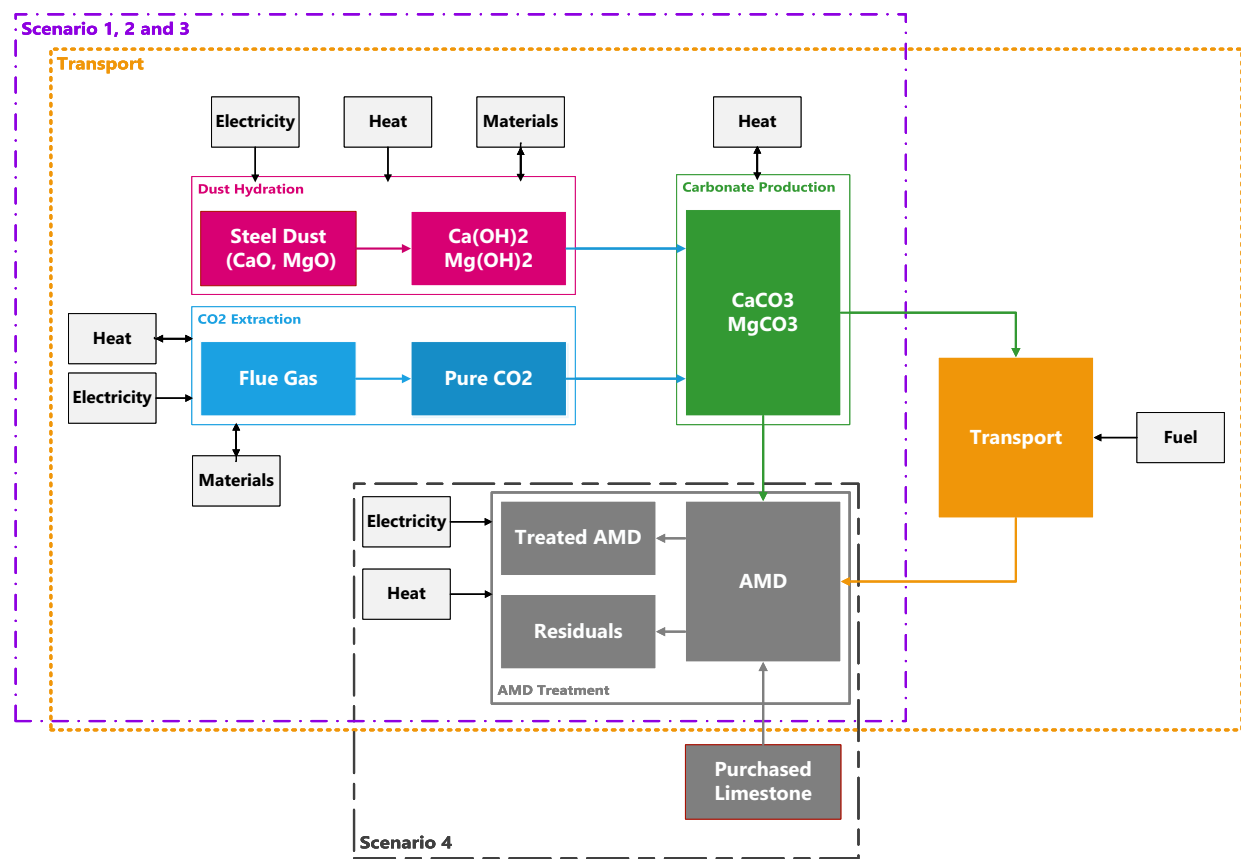


**Fig. 2** System boundaries used in different scenarios of this study

the Golgohar complex. However, the transportation of materials from the UAE to the south of Iran, where the mines are located, was deliberately excluded because the greenhouse gas emissions from shipping are minimal and thus considered negligible. This exclusion was made to focus solely on assessing the effect of the disparity in dust composition. Table 3 presents the composition of the dust stream used from this plant. It should be noted that, similar to the baseline scenario, it was assumed that the iron present in this dust had been separated through a process before use.

#### Scenario #4: Use of Limestone (Conventional Method)

This scenario assessed the traditional approach for treating AMD with limestone. The goal was to contrast the carbon footprint of AMD treatment using the mineralization approach described in earlier scenarios with the conventional method, which involves acquiring pure purchased limestone for AMD treatment. The selected amount,  $\approx 230$  kg, of limestone was calculated based on the calcium carbonate equivalent (CCE) (Moore et al. 1987) of  $\text{CaCO}_3$  and  $\text{MgCO}_3$ . The scenario's system boundary is shown in Fig. 2.

#### Sensitivity Analysis #1: Use of Trucks for Carbonate Transportation

This sensitivity analysis, which was based on the baseline scenario, examined the transportation of carbonates produced from the mineralization stage to remote areas for the treatment of AMD produced in other mines. In other words, the fourth stage of simulation (AMD treatment) designed in the baseline scenario was performed in a different location than the first three sections. Since the amounts of carbonates produced by steel dust is much greater than the amount required for AMD treatment in the same mine, we considered transporting these materials for AMD treatment at other mine sites. The effect of transportation distance on the carbon footprint was considered by selecting trucks with capacities between 16 and 32 tons (small trucks), and more than 32 tons (large trucks). The trucks used in the simulation were conducted with Euro 3 fuel standard, which produces more emissions than newer models using Euro 4 and Euro 5 fuel standards (May et al. 2013; Tzamkiozis et al. 2010); however, they are the most commonly used trucks in the country.

**Table 3** Characteristics of the steel dust of the Emiares steel plant (El-Naas et al. 2015)

Compound	Value (kg)
$\text{SiO}_2$	12.12
$\text{MgO}$	13.38
$\text{CaO}$	108.49

#### Sensitivity Analysis #2: Using Different Amounts of AMD

This sensitivity analysis, which is based on the baseline scenario, examined using different amounts of AMD in the fourth stage, as different AMD volumes with similar specifications can affect the overall carbon footprint. It should be noted that the default amount of AMD in the first scenario was 250 kg. This sensitivity analysis helps determine the quantity of AMD required to keep the process within a carbon-negative range.

### Results and Discussion

This section covers the presentation and discussion of the simulation results, scenarios, and sensitivity analyses that were previously examined, which can be considered as the interpretative stage of the LCA. First, the results of the simulation for treating the AMD will be presented, and subsequently, the results of the scenarios and sensitivity analyses, which were performed in SimaPro software, will be discussed. All the carbon footprint results mentioned throughout the paper were calculated per functional unit, which represents 100 kg of the  $\text{CO}_2$  obtained from flue gas.

#### Results of the Simulation

The final output streams (G3- and SLD) of the simulated model are presented here to demonstrate the effectiveness of the model for using relevant data in the subsequent process. As is evident from Table 4, almost all of the non-standard AMD compounds were eliminated by reactions with the alkaline residues, which increased the pH. This change can be observed by the G3 stream, which represents the treated AMD stream, and the SLD stream, which is made up of the remaining solid materials. The precipitation of  $\text{Fe}^{2+}$  and  $\text{Cu}^{2+}$  ions as  $\text{Fe}_2\text{O}_3$  and  $\text{Cu}_2\text{O}$  is one such example. The mass balance results for the main streams,  $\text{CO}_2$  extraction, dust hydration, carbonate production, and AMD treatment steps are shown in supplemental tables S-2, S-3, S-4, S-5, and S-6, respectively. In addition, the consumed and generated heat and electricity for each step is shown in supplemental Fig. S-1.

#### Results of the Scenarios and Sensitivity Analyses

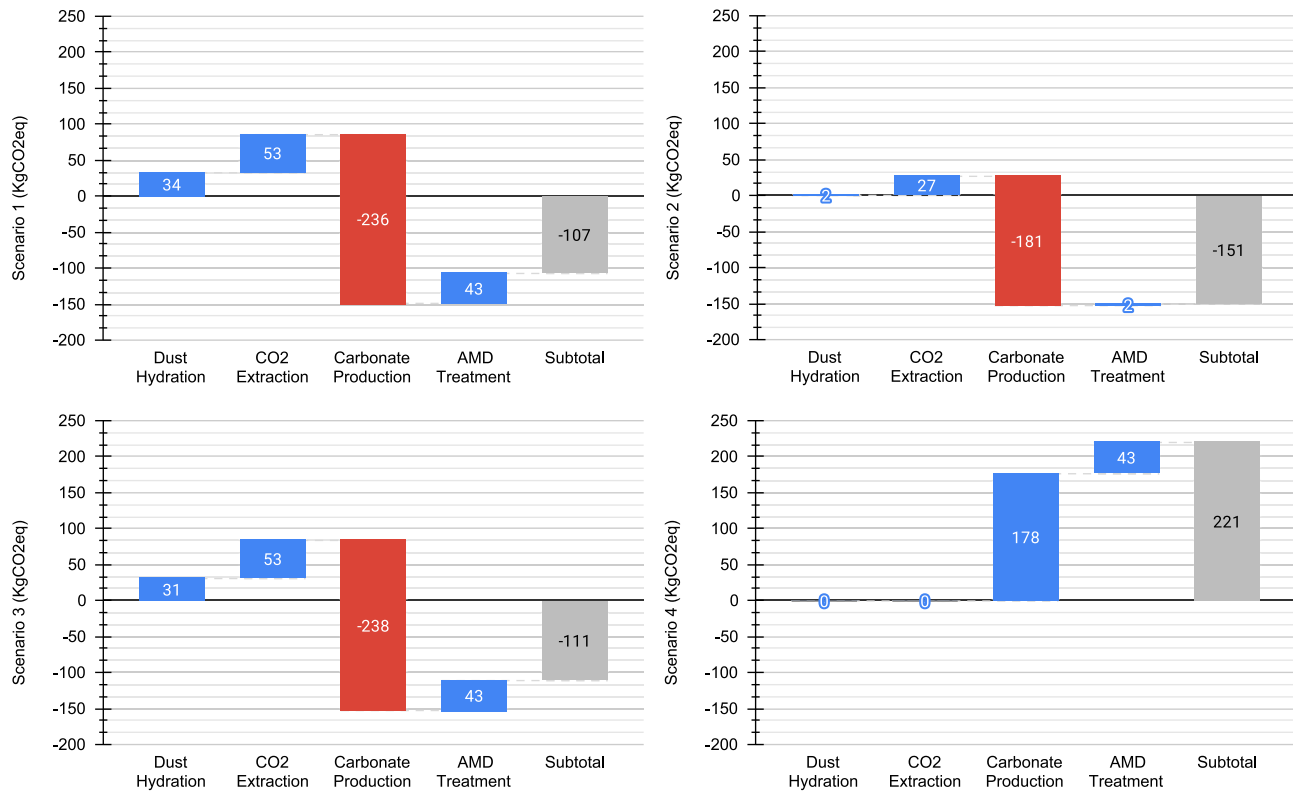
In the first scenario, the overall carbon footprint was  $-107$  kg of  $\text{CO}_2\text{eq}$  (Fig. 3). In the dust hydration step, 34 kg of  $\text{CO}_2\text{eq}$  was emitted, mostly for providing the heat for the reactions and subsequently for the electrical needs of the various equipment. Since salt water is a waste in the Golgohar complex, the use of materials and their upstream carbon

**Table 4** Characteristics of the output streams of the AMD treatment stage

Compounds	SLD (kg)	G3- (kg)
H <sub>2</sub> O	0	249.66
CO <sub>2</sub>	0	$3 \times 10^{-3}$
CO	0	$2.3 \times 10^{-28}$
H <sub>2</sub>	0	$3.35 \times 10^{-19}$
H <sub>2</sub> SO <sub>4</sub>	0	$2.25 \times 10^{-31}$
HCl	0	$3.44 \times 10^{-5}$
SiO <sub>2</sub>	118.28	0
Fe <sub>2</sub> O <sub>3</sub>	$45 \times 10^{-4}$	0
Cu <sub>2</sub> O	$4 \times 10^{-3}$	0
CaCO <sub>3</sub>	50.41	0
CaCl <sub>2</sub>	0.76	0
CaSO <sub>4</sub>	0.53	0
Mg(OH) <sub>2</sub>	2.89	0
MgCO <sub>3</sub>	149.29	0
NaCl	1.15	0
KCl	$21 \times 10^{-4}$	0
Mn <sub>3</sub> O <sub>4</sub>	$7 \times 10^{-4}$	0

footprint is considered zero at this step. The CO<sub>2</sub> extraction was identified as the most GHG emitting stage, as 53 kg of CO<sub>2</sub>eq was released into the atmosphere. The use of various

materials, such as monoethanolamine and water, contributed to the process. However, the energy consumption to provide the necessary heat for the reaction and the required electricity during the process played an even more important role. In the third stage, 236 kg of CO<sub>2</sub>eq was stored, of which most (178 kg of CO<sub>2</sub>eq, Fig. 4) is attributed to the production of carbonate products as an avoided impact, and the remaining amount is considered to store the heat produced by exothermic reactions. In the last step (AMD treatment), 43 kg of CO<sub>2</sub>eq was released, almost all of which was related to providing the necessary heat for the reaction between the AMD and the carbonates obtained from the previous steps. The overall carbon footprint of the heat of reactions, use of various materials in different steps and required electricity for equipment are ranked in the first to third positions, respectively, with 46 kg, 21 kg, and 5 kg of CO<sub>2</sub>eq. (Fig. 4) However, the production of carbonates with a carbon footprint of – 178 kg of CO<sub>2</sub>eq reduces the total value in this scenario to an acceptable amount of – 107 kg of CO<sub>2</sub>eq. The results in this case can be compared to what Ostovari et al. (2020) found in their study. They figured out that using steel slag, which is similar to the steel dust we used in our study, results in about 1.05 tons of CO<sub>2</sub>eq/ton CO<sub>2</sub> stored in the state-of-the-art scenario and 3 tons of CO<sub>2</sub>eq/ton CO<sub>2</sub> stored in the idealized scenario. It's important to mention that the way pure CO<sub>2</sub> is obtained differs between these two studies.

**Fig. 3** Carbon footprint for different stages across four scenarios

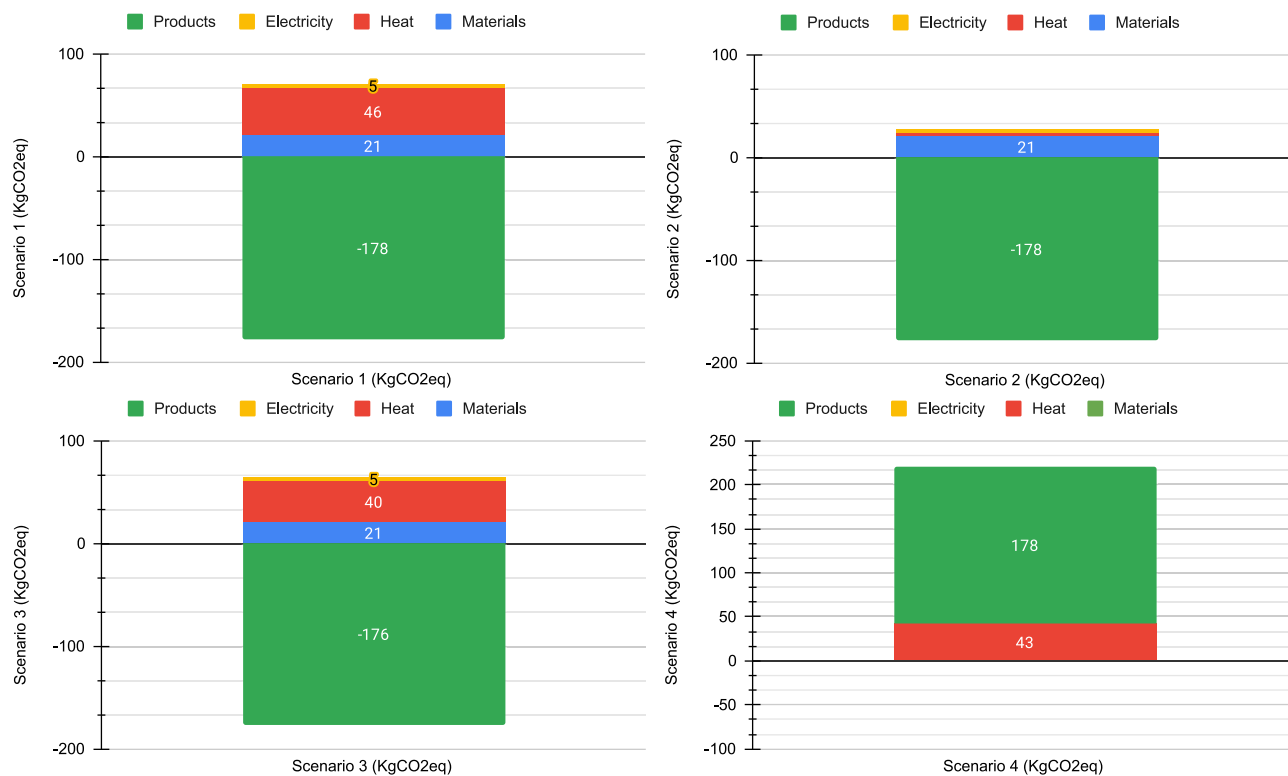


**Fig. 4** Carbon footprint associated with products, materials, electricity, and heat across the four scenarios

Additionally, the final results of the current study involve AMD treatment, which affects the overall carbon footprint. The results for the share of different GHGs in the overall carbon footprint are shown in supplemental Table S-7.

The results of the second scenario show a marked enhancement when compared to the baseline scenario, as the total carbon footprint reaches  $-151$  kg of CO<sub>2</sub>eq (Fig. 3). This remarkable accomplishment is due to the utilization of solar energy to provide the necessary heat for the reaction, rather than using conventional fuels, which produced large amounts of GHG emissions in the previous scenario. In the dust hydration step of this scenario, only 2 kg of CO<sub>2</sub>eq is released to the atmosphere, which is very acceptable compared to the 34 kg of CO<sub>2</sub>eq emission of the previous scenario. This is due to the high efficiency of using solar energy to generate the necessary heat for reactions; since most of the released GHG emissions in this step were related to supplying heat, this scenario had the greatest impact on reducing the carbon footprint of this step. In the CO<sub>2</sub> extraction step, the overall carbon footprint was also halved compared to the first scenario, with a total of 27 kg of CO<sub>2</sub>eq. The remaining amount is mostly attributed to the use of materials and the required electricity for operating the equipment, and only a negligible amount is related to the heat generated from solar energy. The carbon footprint of the carbonate production step, however, reached  $-181$  kg of CO<sub>2</sub>eq, which can be

mostly attributed to the avoided impacts of carbonate products. In the final AMD treatment step, we also see a reduction in GHG emissions similar to the first step, due to the use of solar energy to generate heat for reactions. Figure 4 illustrates a negligible contribution of reaction heat compared to the first scenario, which demonstrates that using solar energy to supply heat for reactions can increase the efficiency of the entire process, even if the carbon footprint of other sources such as consumables and electricity remains constant. While the initial investment required for implementing solar energy systems may be higher, the long-term benefits of a reduced carbon footprint can justify the initial expense (Bhandari et al. 2015; de Wild-Scholten 2013). Results for the share of different GHGs in the overall carbon footprint are shown in supplemental Table S-8.

The results of the third scenario, in which a higher alkalinity dust mixture was used, are shown in Fig. 3. The overall carbon footprint in this scenario was  $-111$  kg of CO<sub>2</sub>eq, which is not as low as the second scenario, although it is still better than the baseline scenario. During the dust hydration step, 31 kg of CO<sub>2</sub>eq was released into the atmosphere, which is about 3 kg of CO<sub>2</sub>eq less than in the first scenario since there was less heat used during this stage. The carbon footprint of the second and fourth steps, namely CO<sub>2</sub> extraction and AMD treatment, are exactly the same as the first scenario; the main difference was in the carbonate

production stage, which was slightly better than the previous two scenarios. This difference was mostly related to the reduced energy consumption during this process and less to the increased amount of carbonate products. This can be clearly seen in Fig. 4, where the carbon footprint due to the production of carbonates (-176 kg of CO<sub>2</sub>eq) was approximately equivalent to the first scenario (-178 kg of CO<sub>2</sub>eq); however, the carbon footprint due to the heat of reactions shows a lower amount (40 kg of CO<sub>2</sub>eq vs. 46 kg of CO<sub>2</sub>eq). It can be concluded that using dust with a greater alkalinity, while leading to more energy storage, also provided a suitable amount of product and reduced the overall carbon footprint of the process. Results for the share of different GHGs in the overall carbon footprint are shown in supplemental Table S-9.

In the fourth scenario, where limestone was replaced with the first three steps of carbonate production, 221 kg of CO<sub>2</sub>eq was released to the atmosphere (Fig. 3). This huge difference demonstrates the efficiency of the first three scenarios compared to the current conventional method. In this scenario, the carbon footprint attributed to limestone production was 178 kg of CO<sub>2</sub>eq (Fig. 4), which is very important. In the AMD treatment stage, the carbon footprint was similar to the first scenario, and the reason for this was the use of the same amounts of AMD and limestone. As can be predicted and seen in Fig. 4, in this scenario, negligible amounts of electricity were utilized, and the final carbon footprint only includes the production of purchased carbonates and the heat used for their reaction with AMD. Results for the share of different GHGs in the overall carbon footprint are shown in supplemental Table S-10.

The results of the first sensitivity analysis show a strong dependence on the carbon footprint of transporting the carbonate products as well as the size of trucks used. Using small trucks with a capacity of 16–32 tons (blue line in Fig. 5), we found that before reaching about 650 tkm (ton-kilometer), which is equivalent to transporting 10 tons of product a distance of 65 km, the total carbon footprint transitioned from the negative range to the positive range (blue dot in Fig. 5). For 1000 and 2000 tkm, the carbon footprint reached 58.5 and 224.1 kg of CO<sub>2</sub>eq, respectively. The large-capacity trucks (red line in Fig. 5) were superior; the point at which the total carbon footprint became zero (red dot in Fig. 5) rose to about 1175 tkm. In addition, after about 2000 tkm, the carbon footprint reached 74.8, showcasing improved performance than the smaller trucks. Results for the share of different GHGs in the final carbon footprint for both small and large trucks are shown in supplemental Tables S-11 and S-12, respectively.

The location of the Golgohar complex and three other mines that have great potential for producing AMD are shown in Fig. 6. The Darreza mine, the source of the AMD used in this research, is located 126 km from the Golgohar

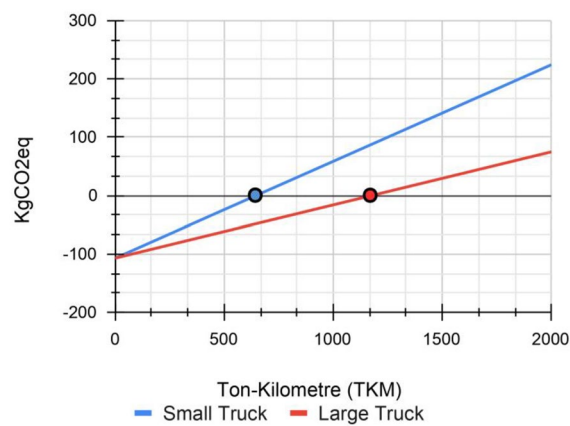


**Fig. 5** The relationship between the carbon footprint and transportation unit (tkm) for two different types of trucks. Dots show the point at which overall carbon footprint becomes zero

complex. Additionally, the Tazareh coal mine and Sungun copper mine are located 1001 km and 1741 km away, respectively. Assuming similar AMD compositions at all three mines, if trucks with Euro3 standard and small size are used to transport the carbonate products obtained in this study for on-site AMD treatment, the carbon footprint of the total process would be –86, 59, and 182 kg of CO<sub>2</sub>eq, respectively. Therefore, even in the most pessimistic scenario, which involves using low-capacity trucks with low fuel standards, the carbon footprint was still in the negative range for transporting products to the Darreza mine. However, the data from the other two mines indicates that this approach achieves carbon-negative results only when the transportation is to the closest locations.

The results of the second sensitivity analysis indicated that different amounts of AMD with similar specifications could markedly affect the overall carbon footprint. The results shown in Fig. 7 indicate that if the amount of the AMD entering the system for treatment was increased from 250 kg, which is similar to the baseline scenario, to 500 kg, the overall carbon footprint, which is mainly due to the increased heat required to carry out the relevant reactions, increases from –107 kg to –64 kg of CO<sub>2</sub>eq. Also, if only 50 kg of AMD is used, the carbon footprint reached a low of –141 kg of CO<sub>2</sub>eq. In addition, if 877 kg of AMD is used for the treatment, the overall carbon footprint reaches zero (the blue dot in Fig. 7) and for larger amounts, it enters the positive range. The results of this scenario show that using steel dust mineralization products to treat large volumes of AMD can still lead to high GHG emissions. Consequently, passive treatment methods with controlled flow rates and acidity loads may be preferable in such cases. For smaller quantities of AMD, however, the novel active treatment method introduced here is a viable option because of its lower infrastructure costs (Trumm

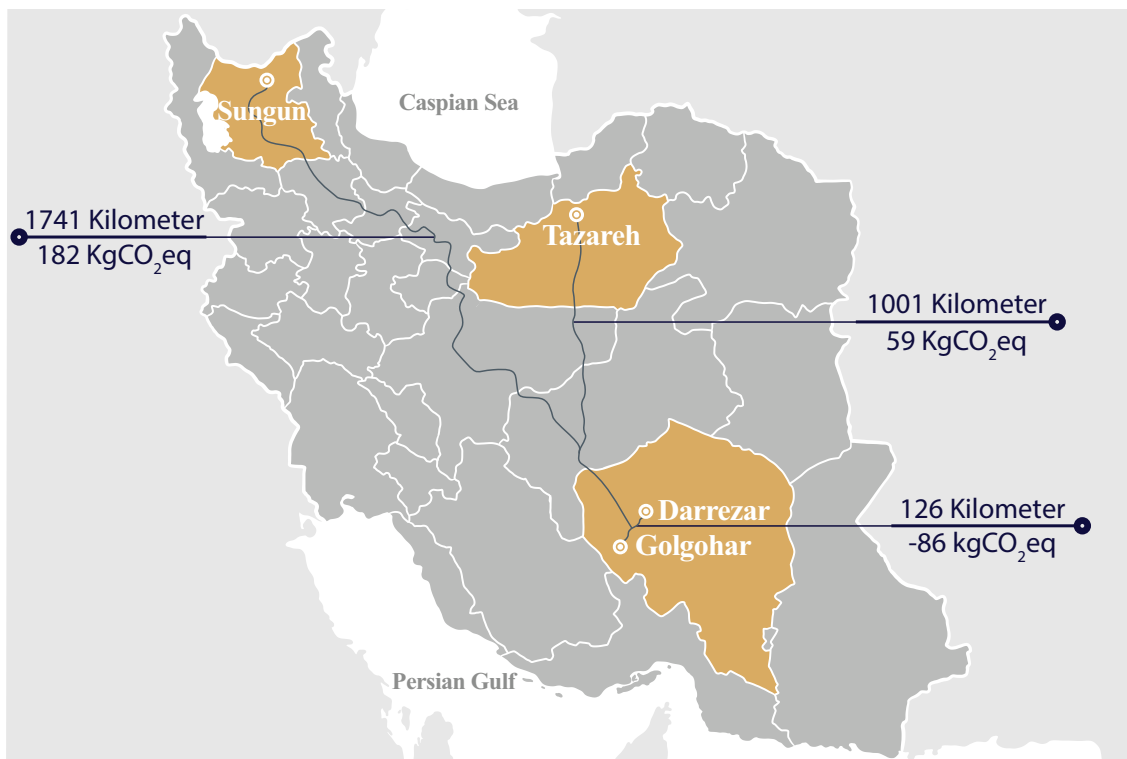


**Fig. 6** The calculated carbon footprint in case the carbonate products are transported to three different mine sites from the Golgohar iron complex (Designed by Freepik)

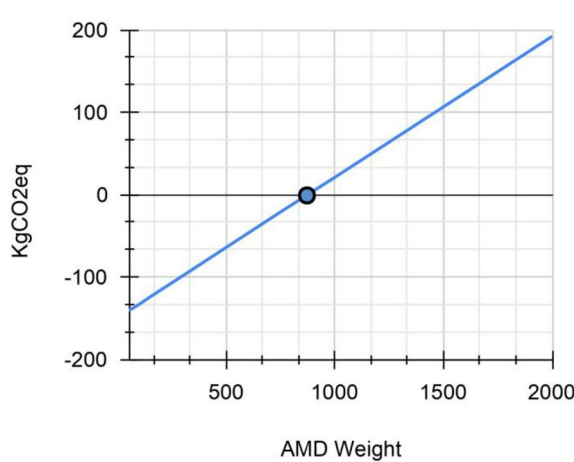


**Fig. 7** The relationship between the carbon footprint and the weight of AMD entered the system for treatment. Blue dot show the point at which overall carbon footprint becomes zero

2010) and negative carbon footprint. It should be noted that conventional active treatment using lime produces much greater GHG emissions due to the process of heating limestone to produce lime, which releases CO<sub>2</sub> (Hengen et al. 2014). GHG results for different amounts of AMD are detailed in supplemental Table S-13.

## Conclusion

Using a LCA approach in combination with simulation, this study investigated the carbon footprint associated with treating AMD using steel dust mineralization products. The simulation methodology deployed a four-step process: CO<sub>2</sub> extraction, dust hydration, carbonate production, and AMD treatment. Each step was carefully simulated, considering material inputs, energy consumption, chemical reactions, and resulting outputs. The simulation outcomes served as a dataset for subsequent LCA. Moreover, four different scenarios and two sensitivity analyses were utilized to investigate the overall carbon footprint. The results of the first or baseline scenario showed that using steel dust to capture CO<sub>2</sub> while treating AMD can lead to a carbon footprint of - 107 kg of CO<sub>2</sub>eq for every 100 kg of CO<sub>2</sub> obtained from the flue gas. In the second scenario, when solar energy was used as the source of heat, it was possible to enhance the overall carbon footprint to - 151 kg of CO<sub>2</sub>eq per functional unit. The third scenario examined the effects of using a dust with higher alkalinity, and it was determined that this was optimal due to energy savings compared to the baseline scenario. The fourth scenario investigated the carbon footprint of using the equivalent amount of conventionally produced limestone, and it was determined that the GHG emissions was far worse, as in this scenario the

calculated carbon footprint was + 221 kg of CO<sub>2</sub>eq/100 kg of CO<sub>2</sub> obtained from flue gas. The first sensitivity analysis examined the transportation of carbonate products to other mine sites for AMD treatment, and it was determined that using high-capacity trucks for long distances was superior to lower capacity trucks with less efficient fuel utilization. In the second sensitivity analysis, the amount of AMD that can be treated was considered, and it was determined that the approach implemented in this study was highly efficient for low volumes of AMD but greater amounts of AMD, the use of passive treatment methods is preferable. The study recommends that future research prioritize the utilization of real-world conditions and employ more comprehensive LCIA methods to evaluate multiple aspects of the process.

It is also possible to provide suggestions for enhancing the overall accuracy of future research based on the difficulties encountered in this study:

- In this study, the use of reactions and simulations under ideal conditions was advantageous because it allowed a controlled environment for data collection and understanding fundamental processes. It also enabled precise assessments and the simplification of complex systems. However, drawbacks arose because ideal conditions do not accurately reflect real-world scenarios, potentially overestimating efficiency and ignoring critical variability in practical applications. Future research should concentrate on real-world tests to supplement simulations, accounting for variables such as impurities, process variations, and regional differences.
- The emphasis in this study was on measuring the overall carbon footprint, and hence, the IPCC assessment method for measuring equivalent carbon was used. However, it is possible for other parameters, such as the effect of the process on human health, can also be examined by using other evaluation methods such as Recipe. Doing this would require that thorough data be gathered for each stage to accurately assess the various impacts of the entire process.
- This study assumed the use of limestone for both conventional active and passive treatment. However, the use of lime and other chemicals in active treatment needs to be considered along with the various combinations of passive treatment approaches. Therefore, a life cycle assessment of these methods is recommended.
- Steel dust residues were used in this study due to their specific properties such as fineness. However, there are other alkaline residues that can be used for carbon mineralization and AMD treatment. Some of these residues, such as red mud (Sahu et al. 2010; Yadav and Mehra 2021), are produced on a large scale and have major environmental impacts. Therefore, these residues should also be considered in future studies.

**Supplementary Information** The online version contains supplementary material available at <https://doi.org/10.1007/s10230-024-01005-0>.

**Funding** Open Access funding enabled and organized by Projekt DEAL.

**Data availability** All the data utilized in this paper are included within the article and its supplementary file and no additional data is available.

**Open Access** This article is licensed under a Creative Commons Attribution 4.0 International License, which permits use, sharing, adaptation, distribution and reproduction in any medium or format, as long as you give appropriate credit to the original author(s) and the source, provide a link to the Creative Commons licence, and indicate if changes were made. The images or other third party material in this article are included in the article's Creative Commons licence, unless indicated otherwise in a credit line to the material. If material is not included in the article's Creative Commons licence and your intended use is not permitted by statutory regulation or exceeds the permitted use, you will need to obtain permission directly from the copyright holder. To view a copy of this licence, visit <http://creativecommons.org/licenses/by/4.0/>.

## References

Ahmadi MH, Ghazvini M, Sadeghzadeh M, Alhuyi Nazari M, Kumar R, Naeimi A, Ming T (2018) Solar power technology for electricity generation: a critical review. *Energy Sci Eng* 6:340–361. <https://doi.org/10.1002/ese3.239>

Akcil A, Koldas S (2006) Acid mine drainage (AMD): causes, treatment and case studies. *J Clean Prod* 14:1139–1145. <https://doi.org/10.1016/j.jclepro.2004.09.006>

Alamdar P, Nematollahi O, Alemrababi AA (2013) Solar energy potentials in Iran: a review. *Renew Sust Energ Rev* 21:778–788. <https://doi.org/10.1016/j.rser.2012.12.052>

Al-Mamoori A, Krishnamurthy A, Rownaghi AA, Rezaei F (2017) Carbon capture and utilization update. *Energ Technol* 5:834–849. <https://doi.org/10.1002/ente.201600747>

Azadi M, Edraki M, Farhang F, Ahn J (2019) Opportunities for mineral carbonation in Australia's mining industry. *Sustainability* 11:1250. <https://doi.org/10.3390/su11051250>

Bhandari KP, Collier JM, Ellingson RJ, Apul DS (2015) Energy Payback Time (EPBT) and Energy Return On Energy Invested (EROI) of solar photovoltaic systems: a systematic review and meta-analysis. *Renew Sust Energ Rev* 47:133–141. <https://doi.org/10.1016/j.rser.2015.02.057>

Bobicki ER, Liu Q, Xu Z, Zeng H (2012) Carbon capture and storage using alkaline industrial wastes. *Prog Energy Combust Sci* 38:302–320. <https://doi.org/10.1016/j.pecs.2011.11.002>

de Wild-Scholten (Mariska) MJ (2013) Energy payback time and carbon footprint of commercial photovoltaic systems. *Sol Energy Mater Sol Cells* 119:296–305. <https://doi.org/10.1016/j.solmat.2013.08.037>

de Simone Souza HH, de Abreu Evangelista PP, Medeiros DL, Albertí J, Fullana-i-Palmer P, Boncz MA, Kiperstok A, Gonçalves JP (2021) Functional unit influence on building life cycle assessment. *Int J Life Cycle Assess* 26:435–454. <https://doi.org/10.1007/s11367-020-01854-1>

Eftekhari F, Doulati Ardejani F, Amini M, Taherdangkoo R, Butscher C (2023) Enhancing tank leaching efficiency through electrokinetic remediation: a laboratory and numerical modeling study. *Water (Basel)* 15:3923. <https://doi.org/10.3390/w15223923>

El-Naas MH, El Gamal M, Hameedi S, Mohamed A-MO (2015) CO<sub>2</sub> sequestration using accelerated gas-solid carbonation of

pre-treated EAF steel-making bag house dust. *J Environ Manag* 156:218–224. <https://doi.org/10.1016/j.jenvman.2015.03.040>

Endzhievskaya IG, Demina AV, Lavorenko AA (2020) Synthesis of a mineralizing agent for Portland cement from aluminum production waste. *IOP Conf Ser Mater Sci Eng* 945:012062. <https://doi.org/10.1088/1757-899X/945/1/012062>

ISO 14040 (2006) Environmental management—Life cycle assessment—Principles and framework.

Gadikota G (2021) Carbon mineralization pathways for carbon capture, storage and utilization. *Commun Chem* 4:23. <https://doi.org/10.1038/s42004-021-00461-x>

Guo M, Murphy RJ (2012) LCA data quality: sensitivity and uncertainty analysis. *Sci Total Environ* 435–436:230–243. <https://doi.org/10.1016/j.scitotenv.2012.07.006>

Hauschild MZ, Rosenbaum RK, Olsen SI (eds) (2018) Life cycle assessment. Springer International Publishing, Cham

Hengen TJ, Squillace MK, O'Sullivan AD, Stone JJ (2014) Life cycle assessment analysis of active and passive acid mine drainage treatment technologies. *Resour Conserv Recycl* 86:160–167. <https://doi.org/10.1016/j.resconrec.2014.01.003>

Herez A, Ramadan M, Abdulhay B, Khaled M (2016) Short review on solar energy systems. p 030041, <https://api.semanticscholar.org/CorpusID:114909712>. Accessed Apr 2023

Hunt AJ, Sin EHK, Marriott R, Clark JH (2010) Generation, capture, and utilization of industrial carbon dioxide. *Chem Sus Chem* 3:306–322. <https://doi.org/10.1002/cssc.200900169>

Ibrahim M, El-Naas M, Benamor A, Al-Sobhi S, Zhang Z (2019a) Carbon mineralization by reaction with steel-making waste: a review. *Processes* 7:115. <https://doi.org/10.3390/pr7020115>

Ibrahim MH, El-Naas MH, Zevenhoven R, Al-Sobhi SA (2019b) Enhanced CO<sub>2</sub> capture through reaction with steel-making dust in high salinity water. *Int J Greenh Gas Control* 91:102819. <https://doi.org/10.1016/j.ijggc.2019.102819>

Kelemen PB, Aines R, Bennett E, Benson SM, Carter E, Coggon JA, de Obeso JC, Evans O, Gadikota G, Dipple GM, Godard M, Harris M, Ja H, Johnson KTM, Kourim F, Lafay R, Lambart S, Manning CE, Matter JM, Michibayashi K, Morishita T, Noël J, Okazaki K, Renforth P, Robinson B, Savage H, Skarbek R, Spiegelman MW, Takazawa E, Teagle D, Urai JL, Wilcox J (2018) In situ carbon mineralization in ultramafic rocks: natural processes and possible engineered methods. *Energy Procedia* 146:92–102. <https://doi.org/10.1016/j.egypro.2018.07.013>

Kelly KE, Silcox GD, Sarofim AF, Pershing DW (2011) An evaluation of ex situ, industrial-scale, aqueous CO<sub>2</sub> mineralization. *Int J Greenh Gas Control* 5:1587–1595. <https://doi.org/10.1016/j.ijggc.2011.09.005>

Lesser P, Gugerell K, Poelzer G, Hitch M, Tost M (2021) European mining and the social license to operate. *Extr Ind Soc* 8:100787. <https://doi.org/10.1016/j.exis.2020.07.021>

Li L, Jiang Y, Pan S-Y, Ling T-C (2021) Comparative life cycle assessment to maximize CO<sub>2</sub> sequestration of steel slag products. *Constr Build Mater* 298:123876. <https://doi.org/10.1016/j.conbuildmat.2021.123876>

Liu L, Ji H, Lü X, Wang T, Zhi S, Pei F, Quan D (2021) Mitigation of greenhouse gases released from mining activities: a review. *Int J Miner Metall Mater* 28:513–521. <https://doi.org/10.1007/s12613-020-2155-4>

Madadgar S, Doulati Ardejani F, Boroumand Z, Sadeghpour H, Taherdangkoo R, Butscher C (2023) Biosorption of aqueous Pb(II), Co(II), Cd(II) and Ni(II) ions from Sungun copper mine wastewater by chrysopogon zizanioides root powder. *Minerals* 13:106. <https://doi.org/10.3390/min13010106>

Martínez NM, Basallote MD, Meyer A, Cánovas CR, Macías F, Schneider P (2019) Life cycle assessment of a passive remediation system for acid mine drainage: towards more sustainable mining activity. *J Clean Prod* 211:1100–1111. <https://doi.org/10.1016/j.jclepro.2018.11.224>

Martínez-Rocamora A, Solís-Guzmán J, Marrero M (2016) LCA databases focused on construction materials: a review. *Renew Sust Energ Rev* 58:565–573. <https://doi.org/10.1016/j.rser.2015.12.243>

May J, Favre C, Bosteels D (2013) Emissions from Euro 3 to Euro 6 light-duty vehicles equipped with a range of emissions control technologies. *Proc, Internal combustion engines: performance, fuel economy and emissions*. Elsevier, New York, pp 55–65

Metz B, Davidson O, de Coninck HC, Loos M, Meyer LA (2005) IPCC special report on carbon dioxide capture and storage. Prepared by Working Group III of the Intergovernmental Panel on Climate Change, Cambridge, UK and New York City.

Moore TJ, Loeppert RH, West LT, Hallmark CT (1987) Routine method for calcium carbonate equivalent of soils. *Commun Soil Sci Plant Anal* 18:265–277. <https://doi.org/10.1080/00103628709367817>

Moreno-González R, Macías F, Meyer A, Schneider P, Nieto JM, Olías M, Cánovas CR (2023) Life cycle assessment of management/valorisation practices for metal-sludge from treatment of acid mine drainage. *Environ Impact Assess Rev* 99:107038. <https://doi.org/10.1016/j.eiar.2023.107038>

Ostovari H, Sternberg A, Bardow A (2020) Rock 'n' use of CO<sub>2</sub>: carbon footprint of carbon capture and utilization by mineralization. *Sustain Energy Fuels* 4:4482–4496. <https://doi.org/10.1039/D0SE00190B>

Pan S-Y, Chen Y-H, Fan L-S, Kim H, Gao X, Ling TC, Chiang PC, Pei SL, Gu G (2020) CO<sub>2</sub> mineralization and utilization by alkaline solid wastes for potential carbon reduction. *Nat Sustain* 3:399–405. <https://doi.org/10.1038/s41893-020-0486-9>

Rebitzer G, Ekvall T, Frischknecht R, Hunkeler D, Norris G, Rydberg T, Schmidt WP, Suh S, Weidema BP, Pennington DW (2004) Life cycle assessment. *Environ Int* 30:701–720. <https://doi.org/10.1016/j.envint.2003.11.005>

Reddy KJ, John S, Weber H, Argyle M, Bhattacharyya P, Taylor DT, Christensen M, Foulke T, Fahlsing P (2011) Simultaneous capture and mineralization of coal combustion flue gas carbon dioxide (CO<sub>2</sub>). *Energy Procedia* 4:1574–1583. <https://doi.org/10.1016/j.egypro.2011.02.027>

Renou S, Thomas JS, Aoustin E, Pons MN (2008) Influence of impact assessment methods in wastewater treatment LCA. *J Clean Prod* 16:1098–1105. <https://doi.org/10.1016/j.jclepro.2007.06.003>

Rim G, Wang D, Rayson M, Brent G, Park AA (2020) Investigation on abrasion versus fragmentation of the Si-rich passivation layer for enhanced carbon mineralization via CO<sub>2</sub> partial pressure swing. *Ind Eng Chem Res* 59:6517–6531. <https://doi.org/10.1021/acs.iecr.9b07050>

Romanov V, Soong Y, Carney C, Rush GE, Nielsen B, O'Connor W (2015) Mineralization of carbon dioxide: a literature review. *ChemBioEng Rev* 2:231–256. <https://doi.org/10.1002/cben.20150002>

Rosenbaum RK, Hauschild MZ, Boulay A-M, Fantke P, Laurent A, Núñez M, Vieira M (2018) Life cycle impact assessment. In: Hauschild MZ, Rosenbaum RK, Olsen SI (eds) Life Cycle Assessment. Springer International Publishing, Cham, pp 167–270

Ross S, Evans D (2002) Excluding site-specific data from the LCA inventory: how this affects life cycle impact assessment. *Int J Life Cycle Assess* 7:141–150. <https://doi.org/10.1007/BF02994048>

Sahu RC, Patel RK, Ray BC (2010) Neutralization of red mud using CO<sub>2</sub> sequestration cycle. *J Hazard Mater* 179:28–34. <https://doi.org/10.1016/j.jhazmat.2010.02.052>

Sala S, Laurent A, Vieira M, Van Hoof G (2020) Implications of LCA and LCIA choices on interpretation of results and on decision support. *Int J Life Cycle Assess* 25:2311–2314. <https://doi.org/10.1007/s11367-020-01845-2>

Sanna A, Uibu M, Caramanna G, Kuusik R, Maroto-Valer MM (2014) A review of mineral carbonation technologies to sequester CO<sub>2</sub>. *Chem Soc Rev* 43:8049–8080. <https://doi.org/10.1039/C4CS00035H>

Shahabpour J, Keshavarzi B (2006) Study of acid mine drainage in Darrehzar copper deposit and its environmental impacts. Shahid Bahonar Univ of Kerman.

Siyar R, Doulati Ardejani F, Norouzi P, Maghsoudy S, Yavarzadeh M, Taherdangkoo R, Butscher C (2022) Phytoremediation potential of native hyperaccumulator plants growing on heavy metal-contaminated soil of Khatunabad copper smelter and refinery. *Iran Water (Basel)* 14:3597. <https://doi.org/10.3390/w14223597>

Skousen J, Zipper CE, Rose A, Ziemkiewicz PF, Nairn R, McDonald LM, Kleinmann RL (2017) Review of passive systems for acid mine drainage treatment. *Mine Water Environ* 36:133–153. <https://doi.org/10.1007/s10230-016-0417-1>

Skousen JG, Ziemkiewicz PF, McDonald LM (2019) Acid mine drainage formation, control and treatment: approaches and strategies. *Extr Ind Soc* 6:241–249. <https://doi.org/10.1016/j.exis.2018.09.008>

Skousen JG, Sexstone A, Ziemkiewicz PF (2000) Acid mine drainage control and treatment. Ch 6 In: Barnhisel RI, Darmody RG, Daniels WL (Eds), *Reclamation of Drastically Disturbed Lands*. pp 131–168. <https://doi.org/10.2134/agronmonogr41.c6>

Tatomir A, McDermott C, Bensabat J, Class H, Edlmann K, Taherdangkoo R, Sauter M (2018) Conceptual model development using a generic Features, Events, and Processes (FEP) database for assessing the potential impact of hydraulic fracturing on groundwater aquifers. *Adv Geosci* 45:185–192. <https://doi.org/10.5194/adgeo-45-185-2018>

Teir S (2008) Fixation of carbon dioxide by producing carbonates from minerals and steelmaking slags. Helsinki Univ of Technology Faculty of Engineering and Architecture.

Tillman A-M, Ekvall T, Baumann H, Rydberg T (1994) Choice of system boundaries in life cycle assessment. *J Clean Prod* 2:21–29. [https://doi.org/10.1016/0959-6526\(94\)90021-3](https://doi.org/10.1016/0959-6526(94)90021-3)

Trumm D (2010) Selection of active and passive treatment systems for AMD—flow charts for New Zealand conditions. *New Zealand J Geol Geophys* 53:195–210. <https://doi.org/10.1080/00288306.2010.500715>

Tuazon D, Corder GD (2008) Life cycle assessment of seawater neutralised red mud for treatment of acid mine drainage. *Resour Conserv Recycl* 52:1307–1314. <https://doi.org/10.1016/j.resconrec.2008.07.010>

Tzamkiozis T, Ntziachristos L, Samaras Z (2010) Diesel passenger car PM emissions: From Euro 1 to Euro 4 with particle filter. *Atmos Environ* 44:909–916. <https://doi.org/10.1016/j.atmosenv.2009.12.003>

Wang X, Song C (2020) Carbon capture from flue gas and the atmosphere: a perspective. *Front Energy Res*. <https://doi.org/10.3389/fenrg.2020.560849>

Yadav S, Mehra A (2021) A review on ex situ mineral carbonation. *Environ Sci Pollut Res* 28:12202–12231. <https://doi.org/10.1007/s11356-020-12049-4>

Yan Z, Wang Y, Yue H, Liu C, Zhong S, Ma K, Liao W, Tang S, Liang B (2021) Integrated process of monoethanolamine-based CO<sub>2</sub> absorption and CO<sub>2</sub> mineralization with SFGD slag: process simulation and life-cycle assessment of CO<sub>2</sub> emission. *ACS Sustain Chem Eng* 9:8238–8248. <https://doi.org/10.1021/acssuschemeng.1c02278>

Zhang Z, Pan S-Y, Li H, Cai J, Olabi AG, Anthony EJ, Manovic V (2020) Recent advances in carbon dioxide utilization. *Renew Sust Energ Rev* 125:109799. <https://doi.org/10.1016/j.rser.2020.109799>